Influence of Internal Curing and Viscosity Modifiers on Resistance to Sulfate Attack

Dale P. Bentz[a]
Jeffrey M. Davis[b]
Max A. Peltz[a]
Kenneth A. Snyder[a]

[a]Materials and Structural Systems Division
Engineering Laboratory
[b]Materials Measurement Science Division
Material Measurement Laboratory
National Institute of Standards and Technology
100 Bureau Drive, Stop 8615
Gaithersburg, MD 20899-8615 USA
E-mail: dale.bentz@nist.gov

Abstract

Sulfate attack is one of the common degradation mechanisms for concrete in severe environments. While various strategies for minimizing sulfate attack are well recognized, including using an ASTM C150 Type V cement, employing supplementary cementitious materials, and/or reducing water-to-cementitious materials ratio, this paper explores two new approaches for increasing a mortar's resistance to sulfate attack. In internal curing, fine lightweight aggregates (LWA) are pre-wetted to provide additional curing water to maximize cement hydration and enhance the microstructure of the interfacial transition zone. The concurrent reductions in connected porosity should contribute to a reduction in the transport rates of sulfate from the environment into the concrete, while the isolated pores present in the LWA may help to accommodate the formation of expansive degradation products, such as ettringite, without creating substantial stresses and subsequent cracking. In the second approach, previously verified for its efficacy to reduce chloride ingress, a viscosity modifier is added to the concrete mixture to increase the viscosity of the pore solution and thus slow down the ingress of sulfates from the environment. While each approach is observed to significantly reduce the measured expansion of mortar bars in standard ASTM C1012 testing, the best performance is observed when the two are combined together by pre-wetting the LWA with a 50:50 solution of the viscosity modifier in water. With the combined approach, the time for the mortar bars to reach a critical expansion level of 0.05 % was over 80 % longer than that measured for the control mortar specimens. The expansion measurements are supported by accompanying measurements of mortar bar mass and surface resistivity throughout their exposure to the sulfate solution, along with micro X-ray fluorescence imaging and X-ray microtomography analysis of specimens extracted from the mortar bars after 9 months of exposure to the sulfate solution.

Keywords: Durability; internal curing; micro X-ray fluorescence; shrinkage-reducing admixture; sulfate attack; viscosity modifier.

Introduction

Sulfate attack is a common degradation mechanism for concretes in certain geographic locations with the United States [1]. Best practices to minimize the effects of sulfate attack include specifying an ASTM C150 Type V cement [2], replacing a portion of the cement in the concrete mixture with fly ash, and/or reducing the water-to-cementitious materials ratio (*w/cm*) of the concrete mixture, the latter typically producing reduced transport coefficients in the field concrete so as to limit the ingress of sulfates from the surrounding soils. Recently, a new paradigm has been introduced for reducing ionic transport and sorption of concrete by modifying the viscosity and surface tension of the concrete pore solution [3-6]. This new technology has been given the acronym VERDiCT, standing for Viscosity Enhancers Reducing Diffusion in Concrete Technology. While the technology has been shown to reduce the ingress of chloride ions into mortar [4,5] and concrete [6] specimens, a similar evaluation with respect to sulfates has been lacking. It is known that the viscosity modifier alters the dissolution and diffusion of sulfate and other ions during the early-age hydration process [7], so it should have beneficial effects in slowing sulfate ingress over the long term, while also possibly altering the morphology of the precipitates of ettringite that form during conventional sulfate attack.

One of the preferred methods for introducing the viscosity modifier into the mortar or concrete is to pre-wet fine lightweight aggregates (LWA) with a 50:50 solution of the chemical admixture in water [4-6]. In this paper, the viscosity modifier will be introduced both via direct addition to the mixing water and via such pre-wetting of LWA. The performance of a mortar prepared with conventional internal curing (IC) [8], as achieved by pre-wetting the LWA with only water, will also be evaluated. As indicated by the generally exemplary performance of lightweight concrete in severe environments [9], internal curing could increase resistance to sulfate attack, both by enhancing hydration of the cement and by providing some additional available porosity to 'accommodate' expansive degradation products such as ettringite.

The sulfate attack resistance of cement-based materials is typically evaluated using the ASTM C1012 standard test method [10] to measure the expansion of mortar bar specimens, although efforts to reduce specimen size and focus on the evaluation of pastes as opposed to mortars have progressed in recent years [11,12]. Since the present study includes an evaluation of the influence of internal curing, a technology based on replacing a portion of the aggregates in concrete with a lightweight counterpart, evaluations of resistance to sulfate attack will be based on the existing mortar bar tests [10], as opposed to the tests based on pastes that are currently under development.

Materials and Experimental Procedures

Four mortar mixtures were prepared using a locally available ASTM C150 Type I/II cement [2] with a Blaine fineness of 362 m^2/kg and a calculated Bogue phase composition of 52.7 % C_3S, 16.2 % C_2S, 7.3 % C_3A, and 10.1 % C_4AF on a mass basis. According to its millsheet, the cement contains 3.35 % limestone powder by mass. Mortars were prepared with a water-to-cement ratio (*w/c*) of 0.485, by mass, with a 57 % volume percentage (on an air-free basis) of ASTM C778 sand [13] in the control mortar. For the mortar mixture with the shrinkage-

reducing admixture/viscosity modifier (Tetraguard AS20[1]) in the mixing water, 10 % of the mix water was replaced by the liquid chemical admixture. For the mortar mixture with IC, 21.7 % of the sand on a volume basis was replaced with an equal volume of pre-wetted fine LWA of a similar size distribution. The LWA had a measured total absorption of 26.5 % on a dry mass basis, with 90 % of this water released when exposed to a 93 % relative humidity environment. The available internal curing water would thus approximately correspond to an additional 0.10 units of water per unit mass of cement in the mortar. For the mortar mixture with both IC and the viscosity modifier introduced via the pre-wetted LWA, this third set of mixture proportions was maintained, but the water used to pre-wet the LWA was replaced by a 50:50 solution (mass basis) of the viscosity modifier in distilled water, achieving the same overall dosage of the admixture as when it was added directly to the mixing water. A 10 % solution of the admixture exhibits a viscosity approximately 50 % higher than that of distilled water, while its surface tension is decreased by about a factor of two [14]. For a 50:50 mixture, the viscosity is about twelve times that of distilled water, while the surface tension reduction remains at approximately 50 % [6].

Mortar mixing was performed according to the procedures provided in ASTM C305 [15]. Cup weights were used to estimate the air content of each mixture. For the control mortar, mortar with viscosity modifier in the mixing water, mortar with IC, and mortar with both, these estimated air contents were 8.4 %, 5.8 %, 7.1 %, and 3.3 %, respectively. This indicates that the shrinkage-reducing admixture/viscosity modifier had a tendency to produce significantly lower air contents in the fresh mortars, as has been observed previously [16].

For each mixture, eight mortar bars were prepared and evaluated for expansion according to the ASTM C1012 standard test method [10], while cubes prepared in accordance with ASTM C109 [17] were produced for evaluating compressive strength. Both mortar bar and cube specimens were cured in their molds in a sealed container with water on the bottom, the container being placed in an environmental chamber maintained at 35 °C ± 3 °C for the first 24 h (such sealed storage conditions for ASTM C1012 specimens are currently under ballot within ASTM). For the control mortar and the mortar with the viscosity modifier in the mix water, demolding was performed at 24 h, resulting in the breakage of one of the eight mortar bars for the former and five of the eight mortar bars for the latter mixture. To avoid this breakage in the subsequent mixtures, following removal from the environmental chamber at 24 h, the mortar bar and cube specimens remained in their sealed containers stored at 23 °C ± 2 °C for a second 24 h period, being then demolded 48 h after casting. For the subsequent two mortar mixtures processed in this manner, all eight mortar bars were successfully demolded without breakage. As per the ASTM C1012 standard [10], the bars and cubes were subsequently cured at 23 °C in limewater, until the cubes reached a strength level of 20.0 MPa or greater. For the control mortar, mortar with viscosity modifier in the mixing water, mortar with IC, and mortar with both, these curing times were 6 d, 8 d, 5 d, and 6 d, respectively. These times are consistent with previous observations that the viscosity modifier slightly retards the hydration reactions [4,6,7], while internal curing can accelerate them [8]. As per the ASTM C1012 standard [10], once achieving this strength level, the mortar bars were placed into the sulfate solution and their expansions

were measured after exposure periods of 1 week, 2 weeks, 3 weeks, 4 weeks, 8 weeks, 13 weeks, 15 weeks, 4 months, 6 months, and 9 months, with the used sulfate exposure solution being replaced by freshly prepared solution at each measurement time. In addition to the expansion measurements, the mass of each mortar bar specimen (free surface water removed) and its surface resistivity, measured using a 4-point Wenner probe, were also periodically assessed. As mentioned previously, seven mortar bars were evaluated for the control mortar, three for the mortar with the viscosity modifier in the mix water, and eight for each of the two subsequent mixtures.

At an age near nine months, pieces were cut from the central region of several of the bars for each mortar mixture, for evaluation using X-ray microtomography [18]. Typical exposure conditions in the X-ray computed tomography (CT) unit were about 90 kV and 110 µA, using a 0.5 mm Al filter, with a 4.1 s acquisition time for each image. The resultant 3-D data sets each consisted of a cubic volume, 2048 elements on a side, obtained with a linear resolution of 17.1 µm/voxel.

Nine specimens were presented for imaging in the Eagle III (EDAX) micro X-ray fluorescence (µXRF) system. Imaging is accomplished by stepping the stage and addressing a focused X-ray beam to an array of equally spaced points. At each point, a full X-ray spectrum is collected and the elements of interest are integrated over their respective spectral ranges [19]. The per pixel dwell time was determined by first analyzing a random selection of points on the sample. The average count rate of the sulfur (S) channel was 11 counts/s, of which 3 counts/s were background due to incoherent scattering of the incident x-ray beam. For a high quality image, based on previous work for imaging sulfur in concrete [20], it was determined that at least 10 counts were required in each pixel. Thus, the time per pixel was increased to 1.5 s. In addition, a 25 µm thick Al window was used to filter the incoming radiation and remove the portion of the background due to Rayleigh (coherent) scattering. Finally, a vacuum equivalent to 100 Pa was used to improve the count rate in the Al, Si and S regions as these elements are heavily absorbed by atmospheric N_2 and O_2.

Results and Discussion

The measured expansion results are provided in Figure 1. While both the application of VERDiCT in the mix water and IC significantly impacted the results, the combination of the two together exhibited the best overall performance in terms of reducing deleterious expansion. Typically, expansions of either 0.05 % or 0.1 % are used as performance criteria for mixtures being evaluated using the ASTM C1012 standard test method. Based on these two criteria, the performance of the VERDiCT in mix water, IC, and IC-VERDiCT mixtures relative to that of the control mortar are summarized in Table 1, where linear interpolation has been used to estimate the exposure times required for each of the four mixtures to reach expansions corresponding to the prescribed 0.05 % and 0.1 % levels. The numbers in parentheses for the IC-VERDiCT mixture are based on an extrapolation of the 9 month results, using the (assumed linear) expansion rate observed between 6 months and 9 months.
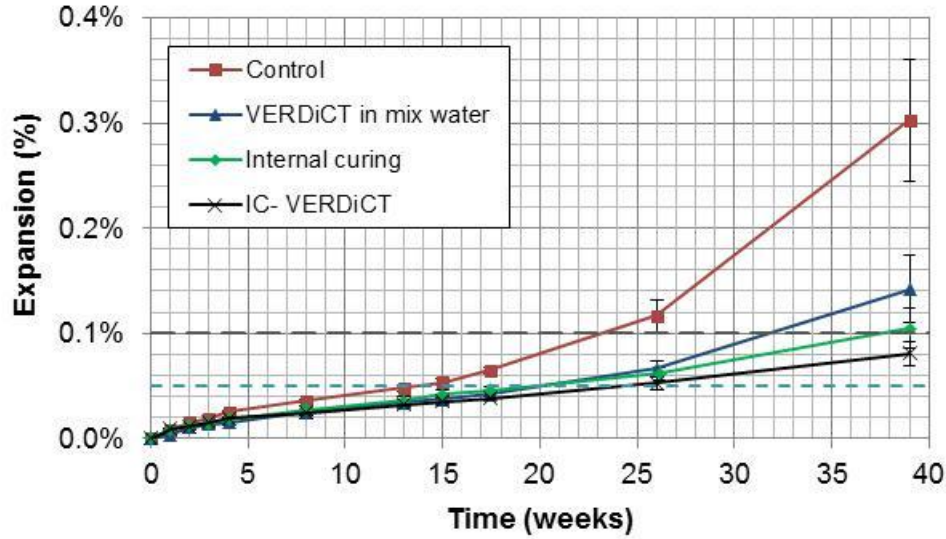
Figure 1. Measured average expansion for mortar bars vs. exposure time in the (replenished) sulfate solution. Error bars indicate ± one standard deviation for the eight (seven for the control and three for VERDiCT in mix water) individual measurements.

Table 1. Estimated exposure times to reach 0.05 % and 0.10 % expansion limits

Mortar	Time to 0.05 % (weeks)	Relative to control	Time to 0.10 % (weeks)	Relative to control
Control	13.5	---	23.5	---
VERDiCT	20	148 %	31.5	134 %
IC	20	148 %	37.5	160 %
IC-VERDiCT	25	185 %	> 39 (48)	> 166 % (200 %)

There are several processes that could be contributing to the observed reductions in expansion. Expansion depends on the diffusion/sorption of sulfates into the mortar bars to react with the interior calcium hydroxide and aluminate phases, to mainly form gypsum and ettringite, respectively [11,12]. Both the incorporation of the VERDiCT admixture into the mortar and the enhanced hydration provided by IC should slow down these diffusion and sorption processes, as has been observed previously in the case of chloride ion penetration [4,5]. In the case of sulfate attack, this could result in a denser layer of reaction products forming on the surfaces of the mortar bars, further reducing subsequent ingress deeper into the specimens. Some evidence for this behavior can be seen in Figures 2 and 3 that show plots of the measured mass changes and the specimen surface resistivities, respectively. For both the VERDiCT in the mix water and the IC mortars, mass gain is reduced relative to the control mortar for exposure ages between 1 week and 4 weeks, while their measured resistivities are generally increasing during the first portion of that same time period. Both of these measures would be consistent with a denser surface layer initially forming in these two sets of specimens. Meanwhile, the control mortar specimens experience a continuous mass gain and little change in their measured resistivity during this time, suggesting a deeper (more uniform) penetration of sulfate ions and accompanying precipitation of expansive reaction products. Surprisingly, the highest mass gain was measured for the IC-VERDiCT combination, but produced little expansion. The presence of the porous LWA, along with the moderate retardation produced by the VERDiCT additive, likely produced a mortar with

a higher initial porosity, allowing for a rapid diffusion/sorption of sulfates during the first few weeks of exposure. Even for this system, though, the rate of mass gain was slowed significantly between 2 weeks and 4 weeks of exposure relative to that measured for the control mortar.
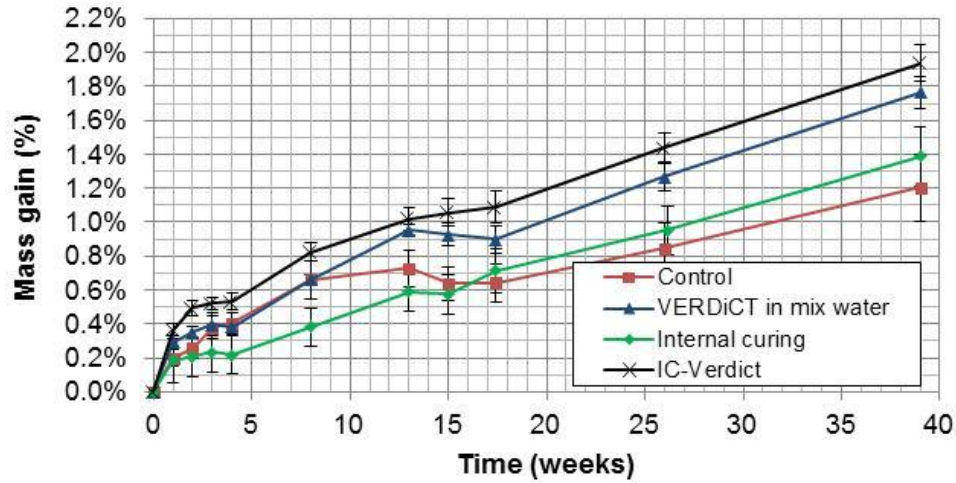

Figure 2. Measured average mass gain for mortar bars vs. exposure time in the (replenished) sulfate solution. Error bars indicate ± one standard deviation for the eight (seven for the control and three for VERDiCT in mix water) individual measurements.
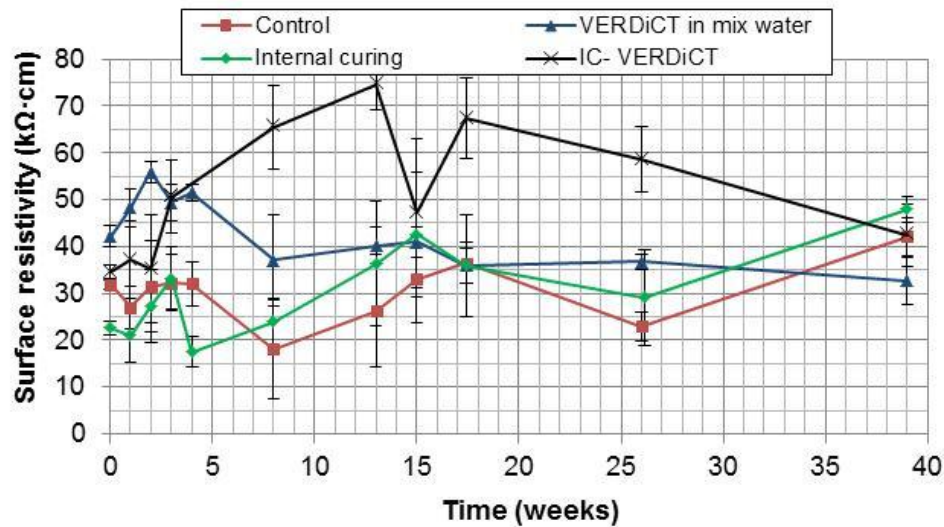

Figure 3. Measured average resistivity for mortar bars vs. exposure time in the (replenished) sulfate solution. Error bars indicate ± one standard deviation for the eight (seven for the control and three for VERDiCT in mix water) individual measurements.

The additional porosity provided by the fine LWA in the IC and IC-VERDiCT mortars may contribute an accommodation mechanism, whereby expansive reaction products first precipitate and grow within the largest (solution-filled) pores present in the mortar microstructure, perhaps including some of those present within the LWA particles, before proceeding to form in the smaller capillary pores within the hydrated cement paste. The expansive stresses and strains would therefore be much less in the systems containing the LWA

for either IC or admixture distribution, leading to less overall expansion, as is indeed observed in Figure 1.

Each of the resistivity vs. time data sets in Figure 3 indicates a somewhat cyclical behavior, with the resistivity increasing and then decreasing again, in a repetitive manner, with nearly all of the measured values remaining within a limited range between 15 kΩ·cm and 50 kΩ·cm for the control, VERDiCT in the mix water, and IC mortars. A likely explanation for this cyclic resistivity response is the ongoing competition between the deposition of sulfate attack reaction products and the damage (cracking) that they produce. At first, available porosity is filled with these reaction products without inducing much expansion/cracking of the specimens. Their reduced porosity leads to an increased resistivity, as measured resistivity is generally controlled by the volume fraction of (pore solution-filled) porosity within the microstructure [21]. However, as the available porosity becomes more filled, the continuing production of expansive degradation products leads to cracking and, in essence, the creation of new, and likely highly connected, porosity. Readily filled by the surrounding conductive solution, these cracks lead to a reduction in measured resistivity (increased conductivity). At this point, a new cycle can begin with the (new) cracks once again being filled by further degradation products and the resistivity rising once more. When damage is extensive, this cyclical pattern can also be observed in the mass loss vs. time curves (Figure 2, from week 8 onwards) as localized extreme damage may result in the loss of pieces (mass) of the mortar bar, followed by a subsequent increase in mass as the sorption/diffusion of sulfate ions and solution into the specimens continues. This is further supported by the general observation of spalling of consecutive (surface) layers that typically occurs during sulfate attack testing.

The resistivity cycle can be modified by both the rate of sulfate ingress and the volume of porosity available to accommodate the expansive reaction products prior to extensive (micro)cracking occurring. As mentioned previously, both VERDiCT and IC should reduce the rate of sulfate ingress, the former by slowing diffusion and sorption rates via the increase in pore solution viscosity (and an accompanying decrease in surface tension [4,5]) and the latter by increasing cement hydration and producing a denser interfacial transition zone (ITZ) microstructure. The combined effects of these two technologies in the IC-VERDiCT mortar produced the mortar with the lowest measured expansion at all ages and also with the most dramatic increase in resistivity during the exposure, nearly reaching 75 kΩ·cm at an age of 13 weeks, before subsequently decreasing to the same level as that exhibited by the other three mortars. In this mortar, there is ample space for the deposition of expansive degradation products, such that a very dense, high resistivity microstructure can be formed, before ultimately succumbing to the never ending and consistently replenished external sulfate solution.

Representative lateral slices from the three-dimensional microtomography data are provided in Figure 4. For the control mortar exposed for nine months, there is ample evidence of both a surface-damaged zone and of internal (micro)cracking, as labeled in Figure 4. For the other three mortars, while a surface-damaged zone could be clearly observed in each case, no evidence of microcracking was found for the specimens examined with the microtomography, consistent with their lower expansion values in Figure 1. As has been observed previously [11,12], damage generally first occurs at the corners (in 2-D, edges in 3-D) of the specimens, with often a portion of one or more of the corners being removed. Generally, the damage layer is
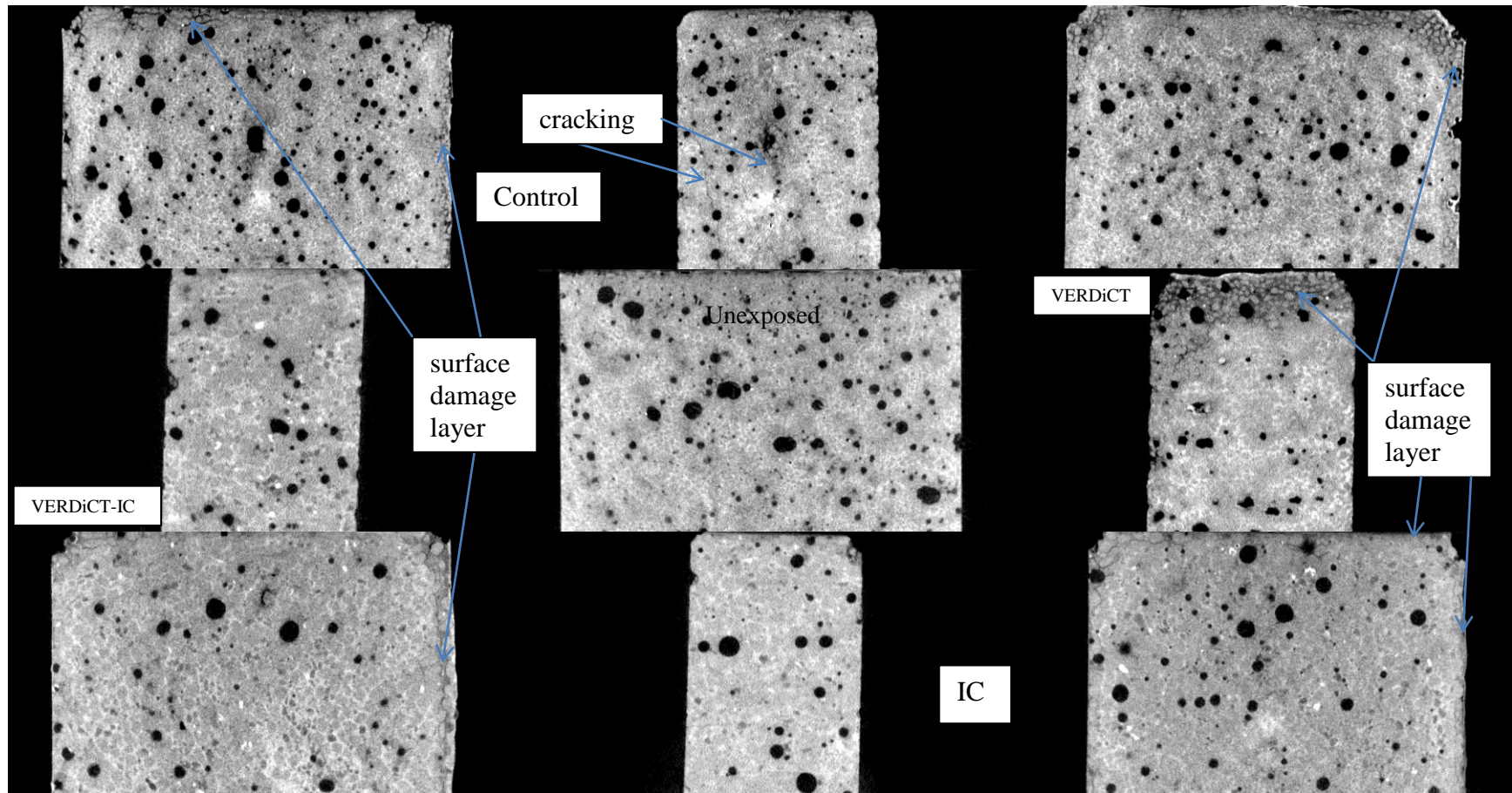
Figure 4. Two-dimensional slices from three-dimensional X-ray microtomography scans of central portions of the original and exposed mortars. The center image is an unexposed control mixture cured in lime water. Proceeding clockwise from the upper left, two images are shown for each of the following exposed mixtures (9 months): control, VERDiCT in the mix water, internal curing (IC), and VERDiCT in the LWA. Original mortar bars were 25.4 mm x 25.4 mm in cross-section. Sliced sections were cut to be approximately 13 mm in thickness.

more prominent on one of the four faces of the extracted specimen, likely corresponding to the finished surface of the original mortar bars. The general lack of air voids within these most damaged surface layers is further evidence that they are likely the finished surfaces of the original specimens.

For the systems with the VERDiCT admixture, either in the mix water or in the LWA, the depth of the surface damage layer appears slightly larger than that for the corresponding two mortars without the admixture (control and IC, respectively). As mentioned previously, the moderate retardation of the hydration by this additive likely produces an initially more permeable mortar, whose surface is more prone to sulfate attack. While the expansion performance of both of these VERDiCT mortars exceeded that of the control at later ages (Figure 1), the microtomography results suggest that further benefits could perhaps be achieved when using the VERDiCT admixture by applying an extended curing time, thus preventing exposure to sulfates until the mortars' microstructure and transport properties have more fully developed.

Color-coded µXRF image maps for elemental sulfur (S) are shown in Figure 5, with all nine images normalized to a single color scale. Areas of highest S concentration are colored in white and yellow, while areas of lower S concentration are colored in red. Areas in black are scaled to the S concentration of the middle (unexposed) specimen. This specimen was not exposed to the sulfate solution, and so its indicated sulfur concentration is entirely from the normal hydration reactions involving gypsum present in the cement powder. While the microtomography images provide a general view of the microstructure and damage of the exposed mortars, the elemental S images highlight the progress of sulfate ingress and its distribution within the mortar bars. Differences are seen among the S distributions for the four mortars, consistent with their measured expansions in Figure 1. For the control mortar, significant sulfate concentrations have reached the center of the specimens after 9 months of exposure. Within a few millimeters of the exposed surface, there is a significant buildup of S, followed by a gradual decline towards the specimen center. This pattern is consistent with scanning electron microscopy observations from previous studies [11,12], the outer zone corresponding to a region where significant leaching of hydration products to create a more porous microstructure (see porosity and damage in Figure 4 also) has occurred. All elements, including S, have been depleted as the capillary porosity of this outer zone is greatly increased. The zone or layer where S is greatest corresponds to a region of the microstructure where the hydrated cement paste has undergone substantial reactions with the ingressing sulfates, gypsum (calcium sulfate dihydrate) replacing calcium hydroxide and unreacted aluminates and previously formed monosulfate phase being converted to ettringite [12]. From this point inward, a typical diffusion front of S into the specimen is observed.

The sulfur distributions are modified by both the VERDiCT additive and IC. Consistent with slowing down the diffusion (and sorption) of sulfate ions, the VERDiCT in the mix water mortar specimens indicate less S reaching the interior of the specimen after the 9 month exposure. However, as mentioned previously, the extent of the (damaged) surface zone is slightly greater, due perhaps to the retardation produced by this additive at early ages, and the maximum concentration of S in zone 2 (gypsum and ettringite formation) appears greater as well.
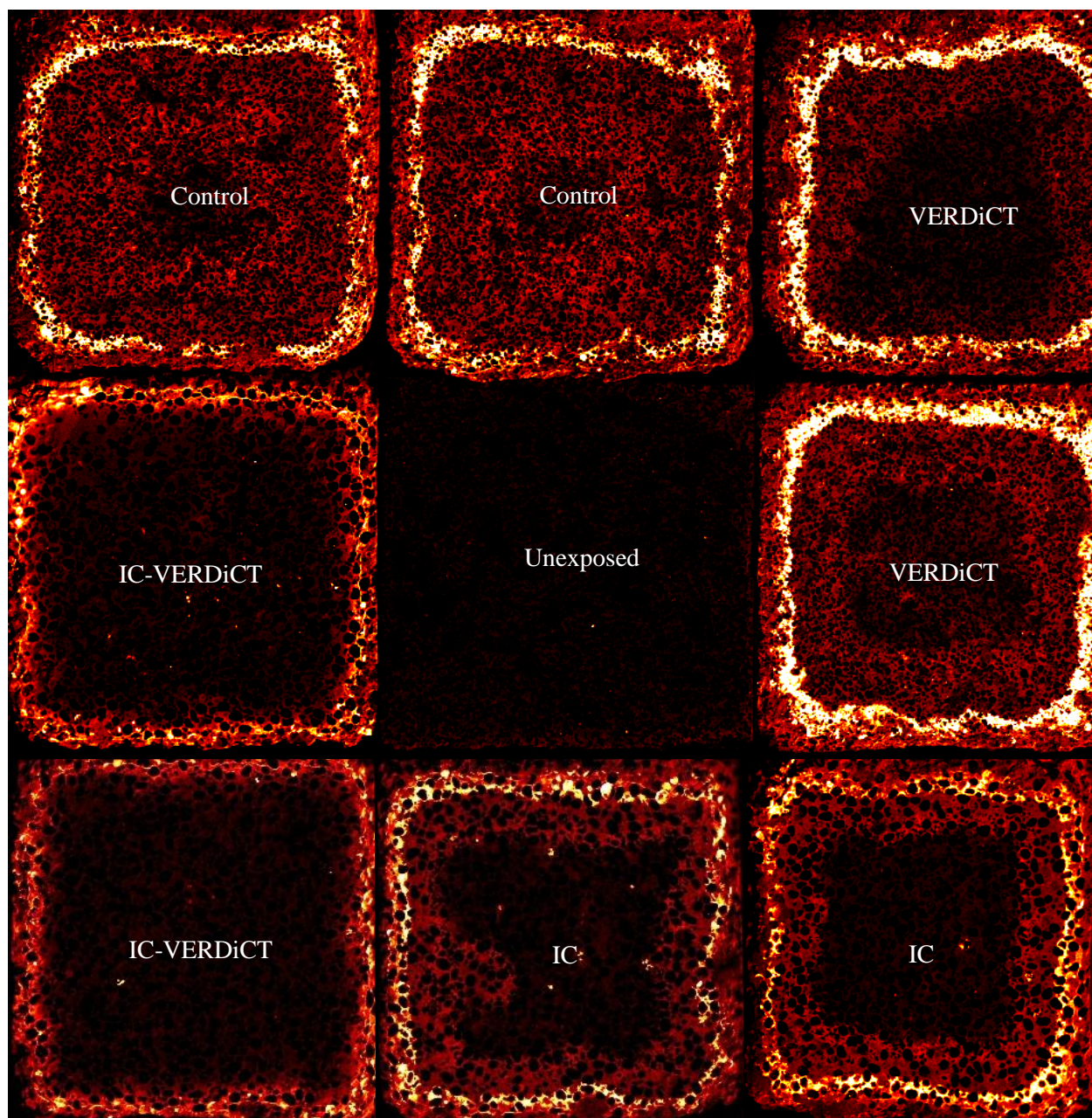
Figure 5. Color-coded (thermal) µXRF images for the elemental S distribution within the exposed (9 months) and control mortar specimens (each 25.4 mm by 25.4 mm). As in Figure 4, proceeding clockwise from the upper left, two images are shown for each of the following exposed mixtures (9 months): control, VERDiCT in the mix water, internal curing, and VERDiCT in the LWA. The central specimen was not exposed to sulfate solution and acted as a control for the image set.

The influence of IC (and VERDiCT-IC) on the sulfate ingress is particularly dramatic in Figure 5 and consistent with the reduced damage observed in Figure 4 for these two mortars. In these systems, the central portion of each specimen exhibits a level of S that is only a little above that observed in the unexposed specimen, indicating that minimal sulfate ions have penetrated to

the specimen center during the 9 month exposure. IC has slowed down the diffusion of the sulfate ions (due to both hydration enhancement and improvement of ITZ microstructure), provided additional space to accommodate any expansive reaction products forming at the surfaces exposed to the sulfate solution, and thus substantially reduced the expansion and its accompanying stress and microcracking (damage). This produces a mortar where sulfates from the surrounding solution do not penetrate to the specimen interior and resistance to sulfate attack is greatly enhanced. The combination of distributing the viscosity modifier via pre-wetting of the LWA (VERDiCT-IC) is shown in Figure 5 to produce a mortar that is clearly superior to the other mortars in terms of minimizing sulfate ingress and thus its accompanying expansion/damage (Figure 1 and Figure 4).

Conclusions

Two new approaches to increasing the resistance to sulfate attack of mortar bars in standardized testing have been evaluated, namely the use of a viscosity modifier (VERDiCT) and the application of internal curing (IC). While each significantly reduced the measured mortar bar expansion over the course of a 9 month exposure, the combination of the two produced a mortar with the best overall performance. Mass and resistivity measurements provided useful additional information to aid in interpreting the expansion trends and the cyclic process of densification and damage that is produced by the expansive (degradation) reactions. The expansion rankings of the four mortars were also consistent with their overall microstructure/damage as observed using X-ray microtomography and the elemental distribution of (ingressing) sulfur as examined using micro X-ray fluorescence. The latter technique is particularly powerful for directly observing the penetration of sulfate ions due to the exposure and could be analyzed further to produce quantitative sulfur distribution maps.

Acknowledgements

References

1) Marchand, J., and Skalny, J.P. (editors), Materials Science of Concrete: Sulfate Attack Mechanisms, American Ceramic Society, Westerville, OH, 1999, 371 pp.

2) ASTM C150-12 Standard Specification for Portland Cement, ASTM International, West Conshohocken, PA, 2012.

3) Bentz, D.P., Snyder, K.A., Cass, L.C., and Peltz, M.A., "Doubling the Service Life of Concrete. I: Reducing Ion Mobility Using Nanoscale Viscosity Modifiers," *Cement and Concrete Composites*, **30** (8), 674-678, 2008.

4) Bentz, D.P., Snyder, K.A., and Peltz, M.A., "Doubling the Service Life of Concrete Structures. II: Performance of Nanoscale Viscosity Modifiers in Mortars," *Cement and Concrete Composites*, **32** (3), 187-193, 2010.

5) Snyder, K.A., Bentz, D.P., and Davis, J.M., "Using Viscosity Modifiers to Reduce Effective Diffusivity in Mortars," *ASCE Journal of Materials in Civil Engineering*, 24 (8), 1017-1024, 2012.

6) Bentz, D.P., Snyder, K.A., Peltz, M.A., Obla, K., and Kim, H., "Viscosity Modifiers to Enhance Concrete Performance," accepted by *ACI Materials Journal*, 2013.

7) Rajabipour, F., Sant, G., and Weiss, W.J., "Interactions between Shrinkage Reducing Admixtures (SRAs) and Cement Paste's Pore Solution," *Cement and Concrete Research*, **38** (5), 606-615, 2008.

8) Bentz, D.P., and Weiss, W.J., "Internal Curing: A 2010 State-of-the-Art Review," NISTIR **7765**, U.S. Department of Commerce, February 2011.

9) Holm, T.A., Bremner, T.W., and Newman, J.B., "Lightweight Aggregate Concrete Subject to Severe Weathering," *Concrete International*, **6**, 49-54, 1984.

10) ASTM C1012/C1012M-12 Standard Test Method for Length Change of Hydraulic-Cement Mortars Exposed to a Sulfate Solution, ASTM International, West Conshohocken, PA, 2012.

11) Ferraris, C.F., Stutzman, P.E., Peltz, M.A., and Winpigler, J.A., "Developing a More Rapid Test to Assess Sulfate Resistance of Hydraulic Cements," *Journal of Research of the National Institute of Standards and Technology*, **110** (5), 529-540, 2005.

12) Ferraris, C.F., Stutzman, P.E., and Snyder, K.A., "Sulfate Resistance of Concrete: A New Approach," R&D Serial No. 2486, Portland Cement Association, Skokie, IL, 2006, 93 pp.

13) ASTM C778-12 Standard Specification for Standard Sand, ASTM International, West Conshohocken, PA, 2012.

14) Sant, G., Eberhardt, A., Bentz, D., and Weiss, J., "Influence of Shrinkage-Reducing Admixtures on Moisture Absorption in Cementitious Materials at Early Ages," *ASCE Journal of Materials in Civil Engineering*, **22** (3), 2010, 277-286.

15) ASTM C305-12 Standard Practice for Mechanical Mixing of Hydraulic Cement Pastes and Mortars of Plastic Consistency, ASTM International, West Conshohocken, PA, 2012.

16) Bentz, D.P., "Capitalizing on Self-Desiccation for Autogenous Distribution of Chemical Admixtures in Concrete," Proceedings of the 4th International Seminar on Self-

Desiccation and Its Importance in Concrete Technology, Eds. B. Persson, D. Bentz, and L.-O. Nilsson, Lund University, 189-196, 2005.

17) ASTM C109/C109M-12 Standard Test Method for Compressive Strength of Hydraulic Cement Mortars (Using 2-in. or [50-mm] Cube Specimens), ASTM International, West Conshohocken, PA, 2012.

18) Bentz, D.P., Martys, N.S., Stutzman, P.E., Levenson, M.S., Garboczi, E.J., Dunsmuir, J., and Schwartz, L.M., "X-ray Microtomography of an ASTM C109 Mortar Exposed to Sulfate Attack," MRS Symposium Proceedings, Vol. 370, Microstructure of Cement-Based Systems/ Bonding and Interfaces in Cementitious Materials, 77-82, 1995.

19) Davis, J.M., Newbury, D.E., Fahey, A., Ritchie, N.W.M., Vicenzi, E.P., Bentz, D.P, "Bridging the Micro-to-Macro Gap: A New Application for Micro X-ray Fluorescence," *Microscopy and Microanalysis*, **17** (3), 410-417, 2011.

20) Davis, J.M., Newbury, D.E., Rangaraju, P.R., Soundarapandian, S., Giebson, C., "Milli X-ray Fluorescence X-ray Spectrum Imaging for Measuring Potassium Ion Intrusion Into Concrete Samples," *Cement and Concrete Composites*, **31** (3), 171-175, 2009.

21) Weiss, W.J., Snyder, K.A., Bullard, J.W., and Bentz, D.P., "Using a Saturation Function to Interpret the Electrical Properties of Partially Saturated Concrete," accepted by *ASCE Journal of Materials in Civil Engineering,* 2013.